Genetic complexity of an obesity QTL (Fob3) revealed by detailed genetic mapping

Incorporating Mouse Genome
Mammalian Genome
Genes and Phenotypes

Genetic complexity of an obesity QTL (*Fob3*) revealed by detailed genetic mapping

Ioannis M. Stylianou,[1,2] Julian K. Christians,[2] Peter D. Keightley,[2] Lutz Bünger,[3] Michael Clinton,[1] Grahame Bulfield,[1,2] Simon Horvat[1,4]

[1]Roslin Institute (Edinburgh), Roslin, EH25 9PS, Scotland, UK
[2]Institute of Cell, Animal and Population Biology, University of Edinburgh, West Mains Road, Edinburgh, EH9 3JT, Scotland, UK
[3]Animal Breeding & Development, Sustainable Livestock Systems, SAC, Bush Estate, Penicuik Midlothian, EH26 0PH, UK
[4]University of Ljubljana, Biotechnical Faculty, Zootechnical Department, Domzale, 1230, Slovenia

Received: 12 September 2003 / Accepted: 26 January 2004

Abstract

Obesity is proving to be a serious health concern in the developed world as well as an unwanted component of growth in livestock production. While recent advances in genetics have identified a number of monogenic causes of obesity, these are responsible for only a small proportion of human cases of obesity. By divergent selection for high and low fat content over 60 generations, we have created Fat (F) and Lean (L) lines of mice that represent a model of polygenic obesity similar to the situation in human populations. From previous crosses of these lines, four body fat quantitative trait loci (QTL) were identified. We have created congenic lines (F^{chr15L}), by recurrent marker-assisted backcrossing, to introgress the QTL region with the highest LOD score, *Fob3* on Chr 15, from the L-Iine into the F-line background. We have further mapped this QTL by progeny testing of recombinants, produced from crosses between the F-line and congenic F^{chrl5L} mice, showing that the *Fob3* QTL region is a composite of at least two smaller effect QTL—the proximal QTL *Fob3a* is a late-onset obesity QTL, whereas the distal *Fob3b* is an early-onset obesity QTL.

Human rates of obesity in the developed world have now reached epidemic levels, and the global number of overweight individuals outstrips the number of underweight cases (WHO 2003). This reflects the effects of a high-fat food culture, combined with a genome evolved to efficiently conserve, partition, and store energy. The human gene map has so far catalogued more than 300 genes, markers, and chromosomal regions that are associated with human obesity (Chagnon et al. 2003). The majority of these are quantitative trait loci (QTL) for obesity or body weight (Bw), mapped primarily in the mouse, as reviewed by Brockmann and Bevova (2002), but also including pigs (Rankinen et al. 2002) and chickens (Van Kaam et al. 1999; Ikeobi et al. 2002; Sewalem et al. 2002). However, very few of these QTL have been mapped beyond the original scan, and given that the intervals of many of these QTL regions are relatively large, the possibility that there may be multiple QTL within those regions has been rarely assessed. It is also unclear how many of the Bw QTL reported are related to obesity and adiposity, since many Bw studies have not involved the further dissection of the 'composite trait' Bw into its components.

A polygenic obesity mouse model would greatly facilitate the studies of the genetics of any complex trait such as obesity. Such a model has been developed in Edinburgh by divergent selective breeding that has resulted in strains differing substantially in fat content (Bünger et al. 2003). The mice were selected for high fat (Fat, F-lines) or low fat (Lean, L-lines) content from a genetically highly variable base population for more than 60 generations (Sharp et al. 1984). Fat content was determined as the ratio of dry matter/body weight after freeze-drying the carcass; the correlation with true fat percentage was 0.98 (Hastings and Hill 1989). From these populations, two inbred lines were produced by eight generations of full-sib matings (Bünger and Hill 1999); the resulting lines differ more than fivefold in fat content and have 22% (F-line) and 4% (L-line) of body

Correspondence to: Simon Horvat, E-mail: Simon.Horvat@bfro.uni-lj.si

fat (Bünger and Hill 1999). Recent research (Bünger et al. 2003) has indicated that polymorphisms in the genes *Lep* (Chr 4) and *Lepr* (Chr 6) have not contributed to the selection response.

A genome-wide QTL analysis using the outbred F and L lines identified four QTL regions for fat content that were significant at a genome-wide level (Horvat et al. 2000): *Fob1* (F-line obesity QTL1), *Fob2*, *Fob3*, and *Fob4* on Chrs 2, 12, 15, and X, respectively. *Fob1*, *Fob2*, *Fob3*, and *Fob4* explained 4.9%, 19.5%, 14.4%, and 7.3% of the F_2 phenotypic variance for fat%, respectively. In the present study, we chose the Chr 15 QTL region (*Fob3*) for further detailed analysis because of its large effect on fat content (it explained 14.4% of the total phenotypic variation) and its strong statistical support (LOD score of 11.3; Horvat et al. 2000). Here we demonstrate successful introgression of the *Fob3* QTL region from the L-line into the F-line. Moreover, through a multiple-QTL analysis, we identify two regions within the original *Fob3* interval, which have significant independent effects, operating in the same direction. In addition, we further characterize the effects of these QTL by analysis of Bw through development, concluding that the two QTL affect the phenotype at different developmental stages.

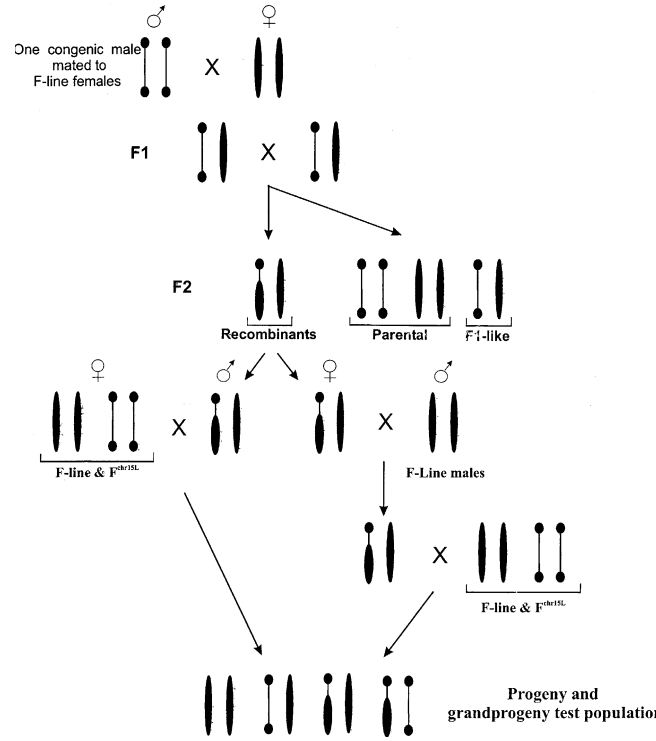

Fig. 1. Mating scheme for generating the progeny from the F_2 mice recombinant within the *Fob3* QTL region. Thin and thick lines indicate chromosomal segments homozygous for the Lean-line and Fat-line alleles, respectively.

Materials and methods

Production of congenic lines and progeny test population. Fat and Lean mouse lines (F-line and L-lines respectively) were selected from a base population, which is based on a cross of two inbred lines (JU and CBA) and one outbred line (CFLP) (Sharp et al. 1984). For a recent review on the F and L-lines, see Bünger and Hill (1999) and Bünger et al. (2003). To develop congenic lines for *Fob3* QTL region, the L-line was crossed to the F-line; then mice heterozygous for the *Fob3* QTL region were selected in each generation and backcrossed five times to the F-line. This produced three congenic sublines termed F^{chr15L}A, F^{chr15L}B, and F^{chr15L}D, collectively termed F^{chr15L} (*F* -line with an *L* *-line segment on chr*omosome *15*). F^{chr15L} A congenic subline, which was later used in a cross to generate recombinants (Fig. 1), has L-line alleles between markers *D15Mit150* and *D15Mit107*; F^{chr15L} B has L-line alleles between *D15Mit184* and *D15Mit39;* and F^{chr15L}D has L line alleles between *D15Mit184* and *D15Mit107* (see Fig. 2 for the map). F^{chr15L}D-line mice were used as the preferred congenic line for all further crosses, while F^{chr15L} A and B-line mice were used where F^{chr15L}D-line mice were in short supply.

At the fifth backcross, L-line alleles at three other QTL found between the F and L-lines on Chr 2, 12, and X [*Fob1*, *2*, and *4* respectively (Horvat et al. 2000)] were selected against. This was done in order to remove any effects associated with these QTL that might have been retained by chance. After the sixth backcross, the estimated F-line background of the congenic line was over 97%.

To fine map the *Fob3* QTL region, recombinants within the *Fob3* region were generated. This was achieved by crossing a single homozygote congenic F^{chr15L} male with nine F-line (inbred) females (Fig. 1). The resulting 42 heterozygous progeny were inter-se mated in order to produce 41 recombinants from 220 progeny. Of these, 23 were male recombinants and were backcrossed to the F-line and congenic F^{chr15L}-line females, to generate 789 progeny from 133 families. The 18 female recombinants were backcrossed first to the F-line males to generate 208 progeny from 35 families. Then selected progeny of the female recombinants possessing the desired recombinant genotype were backcrossed to both F-line and congenic F^{chrI5L}-line mice, generating an additional 182 progeny from 29 families. A general mating scheme is illustrated in Fig. 1.

Microsatellite genotyping. In total, 60 microsatellite markers (Research Genetics) were screened with purified (DNAzol, Life Technologies) spleen

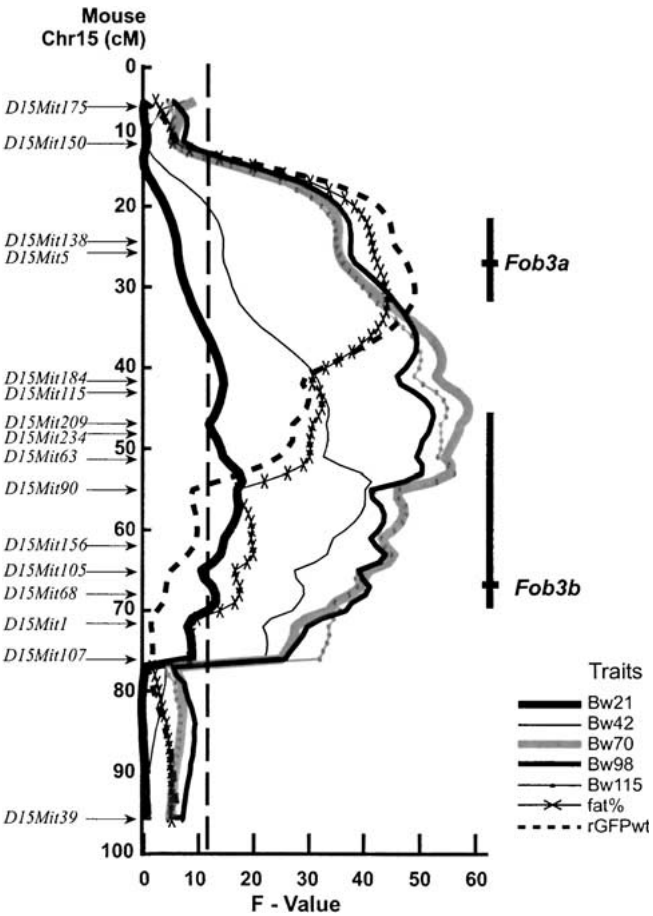

Fig. 2. F-value plots for the single-QTL interval mapping analysis of Bw21, Bw42, Bw70, Bw98, Bw115, fat% and rGFPwt traits. Vertical dashed line indicates significance at the $F_{0.01}$ level. Thick vertical lines with intersections indicate the 95% CI and positions of the peaks for each of the QTL based on the fat% trait multiple QTL analysis.

DNA from a selected set of F and L-line parents. In total, 16 microsatellite mouse markers, polymorphic between the F and L-line alleles on Chr 15, were identified and used in the analysis (Fig. 2).

For general screening of mice, genomic DNA was extracted from mouse ear clips by a modification of the protocol described by Laird et al. (1991). Following incubation of ear clips in 60 μL of lysis buffer, the lysate was diluted 1:40 in distilled water and the resulting solution used as template for PCR. PCR reaction conditions were optimized for each marker's primer set pair in 12 μL final reaction volumes [6 μL diluted lysate (1:40) DNA template, 6 μL 2× PCR premix], with 96-well polypropylene PCR plates (Abgene) on Hybaid JMBS thermocyclers. PCR products were separated on 4% agarose gels (2% MetaPhor agarose, FMC BioProducts, and 2% Agarose MP, Boehringer), with 0.5× TBE buffer containing ethidium bromide (0.5 μg/mL) and loaded with 4 μL of Cresol red loading buffer.

Production of linkage map. Genotypic data for 16 microsatellite markers on Chr 15, spanning four generations, were uploaded into the ResSpecies database [Roslin Institute; http://www.resspecies.org (Law & Archibald 2000)], which checked for pedigree errors based on the genotype of the parents in the previous generation. This data set was analyzed with CriMap (Lander and Green, 1987) to produce a marker map on the basis of observed recombination frequencies. The orders of the markers (Fig. 2) were confirmed by the base pair positions as mapped by the Mouse Genome Sequencing Consortium (MGSC) v 13.30.1 (http://www.ensembl.org/Mus_ musculus/).

Phenotyping. Progeny of recombinant males and grandprogeny of recombinant females were weighed at 21, 42, 70, 98, and 115 days (traits = Bw21, Bw42, Bw70, Bw98, and Bw115 respectively), at which point the mice were euthanized. Male gonadal fat pads (GFP) were removed, weighed, and then replaced in the abdominal cavity. Relative GFP weight (rGFPwt) was expressed as the ratio of the GFP to Bw115. All mice were freeze-dried, and a dry carcass (DM) weight was taken. Percentage body fat (fat%) was calculated as a ratio of Bw115 and DM fitted to a regression equation (below), as described by Hastings and Hill (1989):

$$\text{Predicted fat\%} = (\text{DM}/\text{Bw115}) \times 113 - 30.2 \quad (1)$$

[1] Fat% and Bw are closely correlated in our phenotyped population. The correlation is significant from Bw21 ($r = 0.32$; $P < 0.001$) with an increasing phenotypic correlation over time up to Bw115 ($r = 0.78$; $P < 0.001$).

Single marker analysis. As a first step in the analysis, QTL detection was performed by single marker analysis of variance (ANOVA). This was carried out on 989 phenotyped individuals, using the GLM procedure of the SAS System for Windows Release 6.08 (SAS Institute Inc., Cary, N.C., USA). Each marker was fitted as a fixed effect. For each trait, all 16 markers were analyzed with the model,

$$Y = M + G + L + S + P + S * G + e \quad (2)$$

[2] where M is the trait mean, G is the effect of the genotype (FF, FL, LL), L is the litter effect, S is the sex effect, P is the parity effect (1–2), S*G is the sex-by-genotype interaction, and e is the residual error. For rGFPwt measurements, which were carried out only on males, there was no parity effect detected, so genotype and litter effects only were fitted for this data set.

Single-QTL and Multiple-OTL interval mapping analysis. All traits (Bw21, 42, 70, 98, 115, fat%, and rGFPwt) were examined for normality. This was carried out by using the SAS macro NORMTEST. Additive and dominance coefficients (Haley and Knott 1992) were calculated at 1-cM intervals. These calculations incorporated the progeny's genotypes as well as those of its parents and accounted for the possibility of new recombination within the recombinant parent, but assumed complete interference (i.e., no double recombination within a meiosis). Interval mapping was carried out with a general linear model (proc GLM, SAS Institute, 1989) with a phenotypic trait as the dependent variable and the additive and dominance coefficients as independent variables (Haley and Knott 1992). This model also included parity and sex as fixed effects, and litter size as a covariate. The F-statistics for the additive and dominance coefficients were used as a measure of support for these effects. Significance thresholds were determined empirically by permuting the marker data, as described by Churchill and Doerge (1994). Thresholds were obtained from 1000 permutations and are presented as $F_{0.05}$ and $F_{0.01}$ for significance at $\alpha = 0.05$ and $\alpha = 0.01$, respectively.

All traits were first analyzed by single QTL interval mapping. The strategy for the multiple-QTL analyses was to add QTL to the model until the additional QTL was not significant. Two- and three-QTL analyses were performed by estimating the effects of two or three QTL at separate positions simultaneously, examining all possible pairs or triads of locations (on a 1-cM grid), and selecting the pair, or triad of locations, for which the model explained the most variation. Epistasis was also included in the multiple-QTL analyses. Initially, our "full" linear model for the two-QTL analysis included all epistatic interactions, i.e., additive-by-additive, additive-by-dominance, dominance-by-additive, and dominance-by-dominance interaction terms. We later excluded additive-by-dominance, dominance-by-additive, and dominance-by-dominance terms from the model (see Cheverud et al. 2001) because our preliminary analysis revealed that our experimental design was generally not suitable for estimating interactions involving dominance—our data set contained few or no cases where a family was heterozygous at one position and segregating at another, and hence the *P*-values for the interaction terms involving dominance were undefined. However, the additive-by-additive interaction term was retained in the model if it was found to be significant. If the additive-by-additive term was not statistically significant for a particular trait, it was removed, and the analysis was repeated assuming additivity.

The significance of the additive and dominance effects in the multiple-QTL analyses was assessed by using the threshold F-values determined for a single-QTL analysis. Confidence intervals (CI) for the location of QTL were calculated from 1000 bootstrapped samples (Visscher et al. 1996) assuming there are two QTL. Because bootstrapping of two- and three-QTL analyses would be extremely computationally intensive, we bootstrapped the position of each QTL separately. For example, if a two-QTL analysis identified two QTL, A and B, at locations X and Y respectively, the CI for the position of QTL A would be estimated by performing general linear models with one QTL at position Y and finding the position of a second QTL that maximized the F-value for the entire model; such an analysis would be run for each of the 1000 bootstrap pseudo-samples. The CI for the position of QTL B would then be estimated in a similar way, but by holding the position of one QTL fixed at X. All permutation, bootstrapping and multiple-QTL analyses were performed with SAS.

Results

Single marker (ANOVA) analysis. QTL detection was carried out first using single marker analysis. This was performed on a total of 989 phenotyped progeny and grandprogeny of recombinants. A significant difference ($P < 0.05$) in fat% between the three possible genotypic classes was found at all markers tested, with the exception of *D15Mit175*, *D15Mit150* and *D15Mit39*. This shows that the *Fob3* QTL region was successfully introgressed by marker-assisted backcrossing to the F-line. For the trait rGFPwt in males, a significant difference was observed only at the markers between *D15Mit138* and *D15Mit63*. Single marker analysis of the Bw traits indicates that differences between the genotypic groups become more significant with age and that the differences between the genotypic groups are apparent by 7 weeks of age (data not shown).

Single-QTL interval mapping analysis. All traits except for rGFPwt were approximately normally distributed. A reciprocal transformation was applied to the rGFPwt trait, to achieve greater normality, although a comparison between the interval mapping results of the transformed and untransformed data showed little difference (data not shown).

A summary of the single-QTL analysis for each trait is given in Table 1 and Fig. 2. As originally described by Horvat et al. (2000), the genetic effect of the *Fob3* region (fat% trait), is approximately addi-

tive in nature, i.e., the additive effect is significant ($P < 0.001$), but the dominance effect is not ($P = 0.1$). For Bw115, both the additive and dominance effects are significant at $\alpha = 0.01$. For all other Bw traits, in addition to significant additive effects, there are also significant dominance effects in males, but not in females.

We have used Bw, which is highly correlated to the fat% trait, as an indicator of the development of obesity in our model over time. The results indicate that at weaning age (Bw21), the *Fob3* QTL region is already significant (F-value = 18; $P < 0.001$), indicating that the effect of the *Fob3* QTL region seems to be present early in development. The effect of *Fob3* rises with age from Bw21 and stabilizes at 10 weeks (Bw70), as illustrated by the raw additive effects (Table l) and the standardized additive effects (i.e., divided by the standard deviation for each trait). Beyond 10 weeks, the effect remains approximately at the same level 2.0 g raw additive effect; ~0.4 g standardized additive effect). Figure 2 shows the single QTL analysis plots, for each trait examined, giving the F-value for the additive and dominance terms combined. It can be seen that the peak becomes broader with age, indicating that there may be more than one QTL in the region.

Multiple-QTL Analysis. Multiple QTL analysis was performed on all traits, fitting epistatic interactions (i.e., additive-by-additive) when detected. In the two-QTL analyses the additive-by-additive interaction term for the best pair of locations is significant only for the traits Bw42 and Bw70. In all other cases, no significant interactions were detected, even without correction for multiple tests.

Two significant QTL, designated *Fob3a* and *Fob3b*, were found for most traits except for Bw21 *(Fob3b* only) and rGFPwt *(Fob3a* only). The locations identified in the two-QTL analysis for each trait are summarized in Table 2. For Bw115, *Fob3a* and *Fob3b* mapped to (29cM and 67cM, respectively, and the additive and dominance effects are roughly similar (between 1.2 and 1.5 g) for both QTL (Table 2), and significant in all cases *(Fob3a* additive F = 45.6 vs. $F_{00.1} = 10.9$, dominance F = 13.7 vs. $F_{0.01} = 11.0$; *Fob3b* additive F = 21.5 vs. $F_{0.01} = 10.9$, dominance F = 11.6 vs. $F_{0.01} = 11.0$. The two-QTL analysis of fat% yielded a similar combination of positions, i.e., 27 cM and 68 cM for *Fob3a* and *Fob3b*, respectively (Fig. 3 and Table 2). The estimated additive effect of fat% *Fob3a* is approximately twice (1.62%) that of fat% *Fob3b* (0.71%) and both are significant, though *Fob3b* is significant only at the $\alpha = 0.05$ level *(Fob3a* additive F = 70.7 vs. $F_{0.01} = 11.4$; *Fob3b* additive F = 7.7 vs. $F_{0.05} = 7.4$). The dominance effects are not significant for either of the fat% QTL *(Fob3a* dominance F = 5.1 vs. $F_{0.05} = 7.6$; *Fob3b* dominance F = 5.6 vs. $F_{0.05} = 7.6$). The 95% confidence intervals (CI) for the positions of the two QTL for all the traits, determined by bootstrapping, are presented in Table 2 and shown schematically in Fig. 2 for fat%.

Three-QTL analysis was performed on all traits for which we found two significant QTL. As in the two-QTL analyses, the additive-by-additive interaction terms are not significant in the three-QTL analysis of Bw115 ($P > 0.05$ using threshold F value from single QTL analysis). Without epistasis, the triad of locations that explained the most variation (TMV) for Bw115 is 24–47–67 cM, but the additive and dominance effects of the third QTL (at 47 cM) are not significant (F < 2.0).

In the three-OTL analysis of fat%, however, there is evidence of epistasis. The TMV for fat% is 27–54–63 cM and, as in the two-QTL analysis, the additive effect of the QTL at 27 cM is highly significant (F = 36.3 vs. $F_{0.01}$=11.4), but its dominance effect is not (F = 5.3 vs. $F_{0.05} = 7.6$). The additive(54)-by-additive(63) interaction term is significant for either of these position (F = 10.6 vs. $F_{0.05} = 7.4$), although the additive and dominance effects themselves are not significant for either of these positions (F < 4.0 in all cases). The lack of significance of the two QTL involved in the epistatic interaction is difficult to interpret, although it could be that the two QTL identified in the two-QTL analysis are real, and there is a third locus mapping between the *Fob3a* and *Fob3b*, which is interacting with *Fob3b*.

We found no evidence of three-QTL for Bw98; however, there are three significant QTL for the traits Bw42 and Bw70 with TMVs of 23–28–54 cM and 24–43–66 cM respectively. The TMV for Bw42 had significant additive(23)-by-additive(28) interaction; however, no epistasis was seen in Bw70 in contradiction to our results from the two-QTL analysis in this trait, where we saw significant epistasis.

Discussion

Originally, the *Fob3* QTL region was detected in an F_2 cross as a large effect QTL region with a LOD score of 11.3, and having a two-LOD support interval spanning 10–45 cM. Using an increased number of markers and a congenic line with the *Fob3* region from the L-line introgressed into the F-line background, we have been able to dissect the target *Fob3*

Table 1. Single-QTL interval mapping analysis within the *Fob3* region[a]

	Peak							*Male*		*Female*	
Trait	*cM*	*F-value*	*Additive effect*	*Dominance effect*	*SD*	*Additive effect/SD*	*Sex * additive int (P-value)*	*Additive effect*	*Dominance effect*	*Additive effect*	*Dominance effect*
fat%	31	44.3	2.01 ± 0.22***	0.83 ± 0.43	4.25	0.473	0.97	2.03 ± 0.25***	0.58 ± 0.47	1.97 ± 0.38***	1.24 ± 0.75
rGFPwt	31	49.2	0.51 ± 0.05***	0.25 ± 0.10*	0.77	0.662	N/A	0.51 ± 0.05***	0.25 ± 0.10*	N/A	N/A
Bw115	46	52.6	2.05 ± 0.27***	1.30 ± 0.34***	4.88	0.420	0.061	2.48 ± 0.38***	1.62 ± 0.48***	1.69 ± 0.38***	0.87 ± 0.47
Bw98	53	56.3	2.06 ± 0.27***	1.77 ± 0.36***	4.68	0.440	0.25	2.33 ± 0.39***	2.51 ± 0.51***	1.86 ± 0.38***	1.14 ± 0.50*
Bw70	45	58.9	1.58 ± 0.18***	0.89 ± 0.23***	3.43	0.461	0.0036	2.05 ± 0.27***	1.30 ± 0.34***	1.15 ± 0.23***	0.39 ± 0.30
Bw42	54	42.5	1.09 ± 0.17***	0.83 ± 0.22***	3.02	0.361	0.0055	1.46 ± 0.26***	1.15 ± 0.34***	0.75 ± 0.19***	0.46 ± 0.25
Bw21	54	18.0	0.43 ± 0.12***	0.57 ± 0.16***	2.12	0.203	0.17	0.55 ± 0.17**	0.87 ± 0.23***	0.34 ± 0.17*	0.23 ± 0.23
fat%[b]	34.0	11.3[c]	2.31 ± 0.33	−0.47 ± 0.43							

[a] Effect sizes are not scaled by the standard deviation (SD).
[b] Original data for *Fob3* from Horvat et al. (2000).
[c] Lod-Score.
***$P < 0.001$; **$P < 0.01$; *$P < 0.05$.

Table 2. Multiple-QTL interval mapping analysis within the *Fob3* region

		QTLA (Fob3a)						*QTLB (Fob3b)*					
		Additivity			*Dominance*			*Additivity*			*Dominance*		
Trait	*No. QTL*	*Peak (cM)*	*F-Value*	*Effect[c] ± SE*	*F-Value*	*Effect ± SE*	*CI (cM)*	*Peak (cM)*	*F-Value*	*Effect ± SE*	*F-Value*	*Effect ± SE*	*CI (cM)*
Fat%	2	27	70.7	1.62 ± 0.19	5.1	0.68 ± 0.30	22–32	68	7.7	0.71 ± 0.26	5.6	0.77 ± 0.33	44–70
Bw115	2	29	45.6	1.56 ± 0.23	13.7	1.50 ± 0.41	20–46	67	21.5	1.36 ± 0.29	11.6	1.26 ± 0.37	44–70
Bw98	2	29	39.7	1.49 ± 0.24	9.6	1.28 ± 0.42	22–47	64	17.7	1.26 ± 0.30	18.2	1.59 ± 0.37	47–76
Bw70[a]	3[b]	34	45.3	1.68 ± 0.25	11.3	1.46 ± 0.43	21–46	65	1.1	0.28 ± 0.26	21.1	1.45 ± 0.32	24–75
Bw42[a]	3[b]	28	4.0	0.43 ± 0.21	10.4	0.90 ± 0.28	14–95	54	11.7	0.75 ± 0.22	17.3	1.03 ± 0.25	26–69
Bw21	1	N/A						54	19.5	0.56 ± 0.13	15.3	0.63 ± 0.16	38–68
rGFPwt	1	27	47.3	0.38 ± 0.05	3.1	0.13 ± 0.07	21–38	N/A					

[a] Significant epistasis oetected (Bw42: $F = 7.5$, $P = 0.006$; Bw70: $F = 9.22$, $P = 0.002$).
[b] Evidence of 3 QTL present, although positions are uncertain owing to large overlap in confidence intervals.
[c] Absolute effect sizes given with standard error (SE) and confidence intervals (CI) for QTL locations (cM).

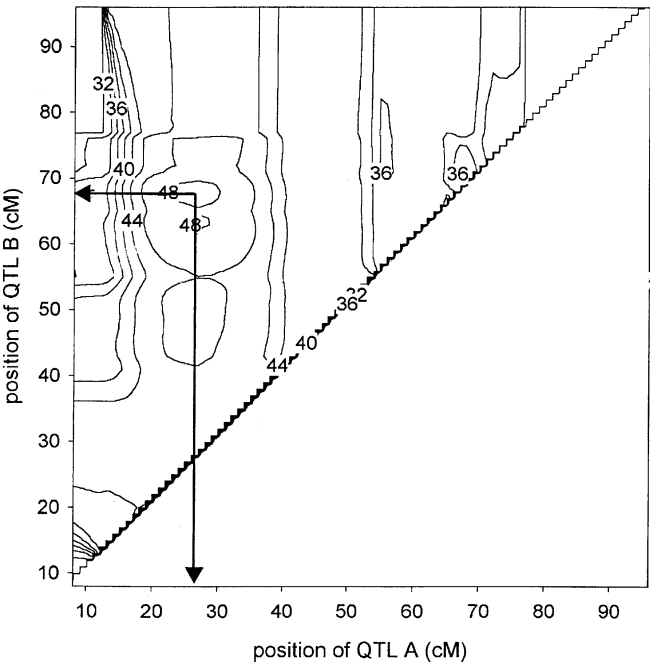

Fig. 3. Contour plot of the two-QTL analysis for fat%. Contour lines indicate the F-value from a general linear model fitting additive and dominance effects for QTL at two positions simultaneously. The "peak" indicates the combination of positions for which the model explains the most variation, and these positions are indicated by the arrows. The contour plot would be symmetrical about the 1:1 line, and therefore only one half of the plot has been shown for clarity.

region (fat% trait) to two smaller QTL, *Fob3a* (27 cM; 22–32 cM;) and *Fob3b* (68 cM; 44–70 cM;). The effects on fat% and Bw115 traits, contributed by each of the QTL separately, are reduced and demonstrate the effect that smaller linked QTL can have in overestimating a single large QTL effect. This has been shown previously *in silico* (Visscher and Haley 1996), and in *in vivo* mouse models (Legare et al. 2000). The importance of carrying out multiple QTL analyses is demonstrated here, as neglecting this may well lead to incorrect conclusions especially in regards to location and effect of the QTL.

We also show through single and multiple QTL analyses that these QTL are closely correlated to Bw and that the effects of the two QTL appear at different developmental stages. QTL for Bw with changing effects over age have been previously identified, for instance by Cheverud et al. (1996), in an F_2 intercross between LG/J and SM/J inbred lines, although in that case there was no indication that the effects were correlated to obesity. Similarly, in an F_2 cross between C57BL/6J × DBA/2J, Morris et al. (1999) and Christians et al. (2003), found a Chr 15 Bw QTL with evidence of increasing effect with age.

We detect *Fob3a* as a late-onset obesity QTL. Although it has a significant effect by 42 days, there is significant epistatic interaction between the two QTL detected, which is still present at Bw70. It is not until the later Bw stages and the fat% trait that it is possible to define this QTL to a 10-cM region (22–32 cM). A significant additive effect was also detected for a correlated trait rGFPwt with a similar 95% CI (21–38 cM), confirming the significant effect *Fob3a* on fat deposition.

Fob3b can be regarded as an early onset obesity QTL, detectable at 21 days, having a 95% CI from 38 to 68 cM, which continues to affect the Bw and fat% traits through development (fat% from 44 to 70 cM) The peak and size of CI for *Fob3b* seem to fluctuate slightly, especially between the early Bw traits, compared with the later traits (Table 2). This is probably due either to the *Fob3a* OTL influencing the analysis or *Fob3b* may itself be a constituent of two QTL with complex epistatic interactions, as indicated by our three-QTL analysis. Interestingly, the related trait rGFPwt is not significant at the *Fob3b* position, indicating that *Fob3b* does not affect the GFP, or that the *Fob3b* QTL also affects fat-free Bw, in addition to obesity. This is reflected in the F-values, which for Bw traits are all significant at the $\alpha = 0.01$ level, whereas fat% reaches significance only at the $\alpha = 0.05$ level.

As mentioned above, *Fob3a* and *Fob3b* had significant additive and dominance effects in Bw traits, but in obesity traits (fat% and rGFPwt), only the additive effects were significant. A possible interpretation could be pleiotropy of *Fob3a* and *Fob3b*—both QTL affect fat tissue mass in an additive manner, but may also affect non-fat tissue mass (e.g., muscle, bone mass), which would be reflected in a composite trait Bw. Although *Fob3a* and *Fob3b* may affect fat tissue in an additive manner, they may also increase non-fat tissue in a dominant manner. In this case no significant effect would be seen in heterozygotes on fat%, but there may be a significant accretion of non-fat tissue mass (i.e., lean/bone) in heterozygotes, resulting in a significant dominance effect for Bw traits. Clearly, a more detailed phenotypic characterization during development coupled with future genetic analyses of *Fob3a* and *Fob3b* would be needed to determine the specificity of *Fob3a* and *Fob3b* on fat tissue mass growth and/or growth of non-fat tissue mass.

Including the *Fob3* region, a total of eight obesity/Bw QTL mapping to mouse Chr 15 have been reported to date. Several of these map proximally to *Fob3a*; the multigenic obesity QTL *Mob4* (Warden et al. 1995) maps at marker *D15Mit13* (3.2 Mb) and hence is likely to be an independent QTL. However,

the diet-dependent QTL *Dob3* and *Dob4* (West et al. 1994; York et al. 1996) peak at marker *D15Nds2* (21.4 Mb), and *Bl/Bw*, a QTL for body length and suggestive for Bw (Mehrabian et al. 1998), have peaks mapping close to the *Fob3a* QTL. Two additional QTL, *Pfat4* and *Pfat5*, have been found on Chr 15; however, markers used were not reported (Pomp 1997). Finally, *Pfat15*, reported by Keightley et al. (1998), was detected as a fat% trait with a peak at *D15Mit29* (74.4 Mb). Further analysis of this QTL (Morris et al. 1999) revealed a two-LOD support interval spanning 44.7 Mb, flanked by markers *D15Mit5* (43.4Mb) *D15Mit159* (8.8 Mb) and thus overlaped with both *Fob3a* and *Fob3a*, potentially being influenced by the same genes.

We carried out a search for candidate genes based on the markers flanking the 95% CIs for the fat% *Fob3a* and *Fob3b* QTL—therefore, a slightly broader interval than the 95% CI was examined. The data given here are taken from the MGSC v.15.30.1 database (http://www.ensembl.org/Mus_musculus), which was searched for genes having their function assigned to metabolism, obesity, or adipogenesis. In the *Fob3a* region spanning interval from *D15Mit150* to *D15Mit184*, there were two such candidates: the cytochrome c oxidase–subunit Vic *(Cox6c)*, which is the terminal enzyme in the respiratory chain (Hofmann et al. 1998), and the thyrotropin-releasing hormone receptor (*Trhr*), which affects obesity via the thyroid hormone pathway (Duthie et al. 1993; Taylor and Rowe 1987). The *Fob3b* QTL interval (between *D15Mit115* and *D15Mit1* contains *Ndufb9* (NADH dehydrogenase (ubiquinone) 1 beta subcomplex, 9), which is involved in the oxidative phosphorylation of NADH to ubiquinone (Gu et al. 1996); Squalene monooxygenase (*Sqle*) involved in the sterol biosynthesis pathway (Kosuga et al. 1995); the myelocytomatosis oncogene (*Myc*, shown to inhibit adipocyte differentiation (Freytag and Geddes 1992); the otoconin 90 precursor (*Oc90*), which was suggested to be involved in lipid catabolism (Wang et al. 1998); thyrotroph embryonic factor (*Tef*), which acts in the thyroid hormone pathway (Drolet et al. 1991); Rho-GTPase-binding protein-1 *(Rhpn1)*, found to bind to the glucose response element and hence triggers genes for lipogenesis (Hasegawa et al. 1999); and finally, diacylglycerol O-acyltransferase-1 (*Dgat1*), which has been shown to be an enzyme in triacylglycerol synthesis (Cases et al. 1998). These candidate genes could be examined in future experiments for differential expression between *Fob3a*/*Fob3b* congenic strains and F line to verify whether any of them could be causal for the QTL effects.

The dissection of the *Fob3* region into at least two QTL reflects the complexity one would expect to see in a polygenically obese population as seen in humans, i.e., many loci having small effects. The challenge to positionally clone such loci is one that must be taken up, if true understanding of the human obesity epidemic is to be achieved. Such future cloning attempts of the two QTL will inevitably be more formidable, since the smaller effects will make the segregation of individual QTL (*Fob3a* and *Fob3b*) harder to track down. Both new QTL intervals are still relatively large, and while candidate genes can be identified, a large proportion of the genomic information pertains to unknown genes. The task to isolate the specific genes responsible for these effects from these intervals is challenging. Ideally, the *Fob3a* and *Fob3b* intervals should be fine mapped further with the ''high resolution genetic mapping'' approach such as using interval-specific congenic strains (ISCS) (Darvasi, 1997). A microarray-based gene expression analysis could be coupled to the fine mapping approach, for instance to examine differences between the F-line and the new ISCS. This could provide a more definitive list of candidates for further investigation and potentially could help elucidate the causal mutations underlying the *Fob3a* and *Fob3b* phenotypic effects and the metabolic pathway(s) involved.

Acknowledgments

We are grateful to Pamela Mackay for help with genotyping the congenic lines and to Adrian White for technical assistance in the mouse facility. This project was supported by a BBSRC grant number 15/G12499 and the BBSRC Roslin Institute core strategic grant.

References

1. Brockmann GA, Bevova MR (2002) Using mouse models to dissect the genetics of obesity. Trends Genet 18, 367–376
2. Bünger L, Hill WG (1999) Inbred lines of mice derived from long-term divergent selection on fat content and body weight. Mamm Genome 10, 645–648
3. Bünger L, Forsting J, McDonald KL, Horvat S, Duncan J et al. (2003) Long-term divergent selection on fatness in mice indicates a regulation system independent of leptin production and reception. FASEB J 17, 85–87
4. Cases S, Smith SJ, Zheng YW, Myers HM, Lear SR et al. (1998) Identification of a gene encoding an acyl CoA:diacylglycerol acyltransferase, a key enzyme in triacylglycerol synthesis. Proc Natl Acad Sci USA 95, 13018–13023

5. Chagnon YC, Rankinen T, Snyder EE, Weisnagel SJ, Perusse L et al. (2003) The human obesity gene map: the 2002 update. Obes Res 11, 313–367
6. Cheverud JM, Routman EJ, Duarte FA, van Swinderen B Cothran K et al. (1996) Quantative trait loci for murine growth. Genetics 142, 1305–1319
7. Cheverud JM, Vaughn TT, Pletscher LS, Peripato AC, Adams ES et al. (2001) Genetic architecture of adiposity in the cross of LG/J and SM/J inbred mice. Mamm Genome 12, 3–12
8. Christians JK, Bingham VK, Oliver FK, Heath TT, Keightley PD (2003) Characterization of a QTL affecting skeletal size in mice. Mamm Genome 14, 175–183
9. Churchill GA, Doerge RW (1994) Empirical threshold values for quantitative trait mapping. Genetics 138, 963–971
10. Darvasi A (1997) Interval-specific congenic strains (ISCS): an experimental design for mapping a QTL into a 1-centimorgan interval. Mamm Genome 8, 163–167
11. Drolet DW, Scully KM, Simmons DM, Wegner M, Chu KT et al. (1991) TEF, a transcription factor expressed specifically in the anterior pituitary during embryogenesis, defines a new class of leucine zipper proteins. Genes Dev 5, 1739–1753
12. Duthie SM, Taylor PL, Anderson L, Cook J, Eidne KA (1993) Cloning and functional characterisation of the human TRH receptor. Mol Cell Endocrinol 95, R11–R15
13. Freytag SO, Geddes TJ (1992) Reciprocal regulation of adipogenesis by Myc and C/EBP alpha. Science 256, 379–382
14. Gu JZ, Lin X, Wells DE (1996) The human B22 subunit of the NADH-ubiquinone oxidoreductase maps to the region of chromosome 8 involved in branchio-oto-renal syndrome. Genomics 35, 6–10
15. Haley CS, Knott SA (1992) A simple regression method for mapping quantitative trait loci in line crosses using flanking markers. Heredity 69, 315–324
16. Hasegawa J, Osatomi K, Wu RF, Uyeda K (1999) A novel factor binding to the glucose response elements of liver pyruvate kinase and fatty acid synthase genes. J Biol Chem 274, 1100–1107
17. Hastings IM, Hill WG (1989) A note on the effect of different selection criteria on carcass composition in mice. Anim Prod 48, 229–233
18. Hofmann S, Lichtner P, Schuffenhauer S, Gerbitz KD, Meitinger T (1998) Assignment of the human genes coding for cytochrome c oxidase subunits Va (COX5A), VIc (COX6C) and VIIc (COX7C) to chromosome bands 15q25, 8q22 → ;q23 and 5ql4 and of three pseudogenes (COX5AP1, COX6CP1, COX7CP1) to 14q22, 16pl2 and 13q14 → ;q21 by FISH and radiation hybrid mapping 141. Cytogenet Cell Genet 83, 226–227
19. Horvat S, Bünger L, Falconer VM, Mackay P, Law A et al. (2000) Mapping of obesity QTLs in a cross between mouse lines divergently selected on fat content. Mamm Genome 11, 2–7
20. Ikeobi CO, Woolliams JA, Morrice DR, Law A, Windsor D et al. (2002) Quantitative trait loci affecting fatness in the chicken. Anim Genet 33, 428–435
21. Keightley PD, Morris KH, Ishikawa A, Falconer VM, Oliver F (1998) Test of candidate gene—quantitative trait locus association applied to fatness in mice. Heredity 81, 630–637
22. Kosuga K, Hata S, Osumi T, Sakakibara J, Ono T (1995) Nucleotide sequence of a cDNA for mouse squalene epoxidase. Biochim Biophys Acta 1260, 345–348
23. Laird PW, Zijderveld A, Linders K, Rudnicki MA, Jaenisch R et al. (1991) Simplified mammalian DNA isolation procedure. Nucleic Acids Res 19, 4293
24. Lander ES, Green P (1987) Construction of multilocus genetic linkage maps in humans. Proc Natl Acad Sci USA 84, 2363–2367
25. Law AS, Archibald AL (2000) Farm animal genome databases. Brief Bioinform 1, 151–160
26. Legare ME, Bartlett FS, Frankel WN (2000) A major effect QTL determined by multiple genes in epileptic EL mice. Genome Res 10, 42–48
27. Mehrabian M, Wen PZ, Fisler J, Davis RC, Lusis AJ (1998) Genetic loci controlling body fat, lipoprotein metabolism, and insulin levels in a multifactorial mouse model. J Clin Investig 101, 2485–2496
28. Morris KH, Ishikawa A, Keightley PD (1999) Quantitative trait loci for growth traits in C57BL/6J × DBA/2] mice. Mamm Genome 10, 225–228
29. Pomp D (1997) Genetic dissection of obesity in polygenic animal models. Behav Genet 27, 285–306
30. Rankinen T, Perusse L, Weisnagel SJ, Snyder EE, Chagnon YC (2002) The human obesity gene map: the 2001 update. Obes Res 10, 196–243
31. SAS Institute (1989) SAS/STAT *User's Guide*, Version 6, 4th, ed, Volume 2 (Cary, NC, SAS Institute Inc.),
32. Sewalem A, Morrice DM, Law A, Windsor D, Haley CS et al. (2002) Mapping of quantitative trait loci for body weight at three, six, and nine weeks of age in a broiler layer cross. Poult Sci 81, 1775–1781
33. Sharp GL, Hill WG, Robertson A (1984) Effects of selection on growth, body composition and food intake in mice. I. Responses in selected traits. Genet Res 43, 75–92
34. Taylor BA, Rowe L (1987) The congenital goiter mutation is linked to the thyroglobulin gene in the mouse. Proc Natl Acad Sci USA 84, 1986–1990
35. Van Kaam JB, Groenen MA, Bovenhuis H, Veenendaal A, Vereijken AL et al. (1999) Whole genome scan in chickens for quantitative trait loci affecting growth and feed efficiency. Poult Sci 78, 15–23
36. Visscher PM, Haley CS (1996) Detection of putative quantitative trait loci in line crosses under infinitesimal genetic models. Theor App Gene 93, 691–702
37. Visscher PM, Thompson R, Haley CS. (1996) Confidence intervals in QTL mapping by bootstrapping. Genetics 143, 1013–1020
38. Wang Y, Kowalski PE, Thalmann I, Ornitz DM, Mager DL (1998) Otoconin-90, the mammalian otoconial matrix protein, contains two domains of homology to secretory phospholipase A2. Proc Natl Acad Sci USA 95, 15345–15350
39. Warden CH, Fisler JS, Shoemaker SM, Wen PZ, Svenson KL et al. (1995) Identification of four chromosomal

loci determining obesity in a multifactorial mouse model. J Clin Investig 95, 1545–1552
40. West DB, Goudey-Lefevre J, York B, Truett GE (1994) Dietary obesity linked to genetic loci on chromosomes 9 and 15 in a polygenic mouse model. J Clin Investig 94, 1410–1416
41. WHO-World Health Organisation. Anonymous. Controlling the global obesity epidemic. (2003 Jun). WHO/NHD/00.6
42. York B, Lei K, West DB (1996) Sensitivity to dietary obesity linked to a locus on chromosome 15 in a CAST/Ei×C57BL/6J F2 intercross. Mamm Genome 7, 677–681